High magnetic field test of the ITER outer vessel steady-state magnetic field Hall sensors at ITER relevant temperature

S. Entler, J. Sebek, I. Duran, K. Vyborny, O. Grover, M. Kocan, and G. Vayakis

Citation: Review of Scientific Instruments **89**, 10J112 (2018); doi: 10.1063/1.5038812
View online: https://doi.org/10.1063/1.5038812
View Table of Contents: http://aip.scitation.org/toc/rsi/89/10
Published by the American Institute of Physics

High magnetic field test of the ITER outer vessel steady-state magnetic field Hall sensors at ITER relevant temperature

S. Entler,[1,a)] J. Sebek,[2] I. Duran,[1] K. Vyborny,[3] O. Grover,[1] M. Kocan,[4] and G. Vayakis[4]
[1]*Institute of Plasma Physics of the CAS, Za Slovankou 1782/3, 182 00 Prague 8, Czech Republic*
[2]*Institute of Physics of the CAS, Na Slovance 1999/2, 182 21 Prague 8, Czech Republic*
[3]*Institute of Physics of the CAS, Cukrovarnicka 10/112, 162 00 Prague 6, Czech Republic*
[4]*ITER Organization, Route de Vinon-sur-Verdon, CS 90 046, 13067 St. Paul Lez Durance Cedex, France*

(Presented 16 April 2018; received 5 May 2018; accepted 24 July 2018;
published online 8 August 2018)

The ITER outer vessel steady-state magnetic field sensor diagnostics consist of sixty sensor units. Each sensor unit features a pair of ceramic-metal Hall sensors with a sensing layer made of bismuth. The sensors were tested simultaneously in the magnetic field ranging from −12 T to +12 T at the temperature range from 27 to 127 °C. The Hall coefficient and magnetoresistance of the bismuth layer related to the sensors were identified. In the sensor operating conditions, the Hall coefficient dependence on temperature was fitted with an exponential function with a relative error of less than 0.08%, and the dependence on the magnetic field was fitted with a Gaussian-like function with a relative error of less than 0.11%. An alternative expression based on the physical understanding of the free charge carrier transport in semimetals was derived to describe the dependence of the Hall coefficient on the magnetic field, and its fitting error of 1.2 mT in terms of the magnetic field measurement has met the ITER measurement accuracy requirements. *Published by AIP Publishing.* https://doi.org/10.1063/1.5038812

I. INTRODUCTION

The outer vessel steady-state sensors (OVSS) constitute a part of the ITER magnetic diagnostics.[1] They will contribute to the measurement of the plasma current, plasma-wall clearance, and low-frequency <10 Hz MHD modes.

Three ITER vacuum vessel sectors separated toroidally by 120° will be instrumented with twenty OVSS units each. The units will be installed on the outer skin of the vacuum vessel[2] (Fig. 1). Each OVSS contains a pair of ceramic-metal Hall sensors with a sensing layer made of bismuth positioned perpendicular to each other to measure the tangential and normal components of the magnetic field (Fig. 2).[3]

The operating magnetic field range will be ±2.5 T with an allowed error of 4 mT in accordance with the ITER measurement requirements. The operating temperature of the sensors will be a few degrees below the vacuum vessel temperature of 100 °C.[2]

In addition, the sensors need to withstand up to 500 vacuum vessel baking cycles up to 220 °C and a total neutron fluence of up to 1.3×10^{22} n/m^2. The measurement is not required during the baking cycles.[2]

The substrate of the Hall sensors is an aluminum nitride ceramic plate with the dimensions of 6.4 mm × 6.4 mm and a thickness of 630 μm, coated on both sides with a copper layer with a thickness of 127 μm. Copper contact pads are etched on one side of the substrate. The bismuth sensitive layer with a thickness of 1 μm is deposited on the substrate by magnetron sputtering. The bismuth layer is passivated by two protective layers of alumina. The first alumina layer consists of a 5 μm coating, whereas the second layer is produced by an Al_2O_3 ceramic paste. Figure 3 shows the final sensor before passivation by alumina.

The sensor output signal is processed by a controller[4] which amplifies the normal Hall voltage and suppresses the planar Hall voltage, the offset voltage as well as the interference voltages. The normal Hall voltage is proportional to the component of B normal to the sensitive layer,

$$V_H = R_H \frac{I}{t} B_N, \tag{1}$$

where R_H denotes the normal Hall coefficient, I is the sensor supply current, B_N is the normal component of the magnetic

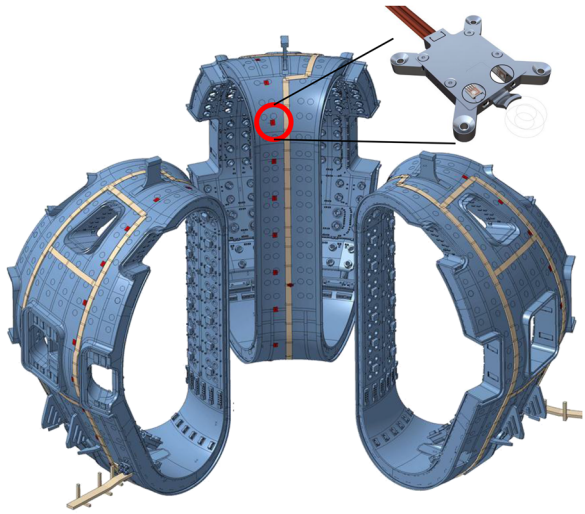

FIG. 1. Poloidally distributed OVSS diagnostic set in the ITER vacuum vessel sectors 2, 5, and 8.

Note: Paper published as part of the Proceedings of the 22nd Topical Conference on High-Temperature Plasma Diagnostics, San Diego, California, April 2018.

a)Author to whom correspondence should be addressed: entler@ipp.cas.cz.

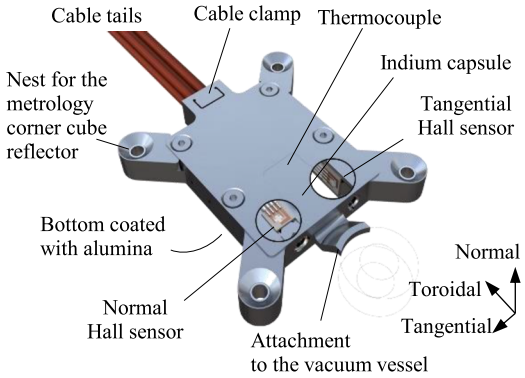

FIG. 2. Outer vessel steady-state magnetic field Hall sensors (OVSS).

field, and t is the sensing layer thickness. The Hall coefficient is inversely proportional to the concentration of free charge carriers in bismuth. As was found in earlier experiments,[5] the bismuth Hall coefficient is exponentially dependent on the temperature and features a Gaussian-like dependence on the magnetic field.

The aim of this paper is to describe the dependence of the Hall sensor output voltage on the magnetic field and temperature using the Hall coefficient in the full range of the sensor operating conditions, i.e., at the magnetic field up to 2.5 T and at temperatures of about 100 °C.

II. EXPERIMENTAL SETUP

The measurements were performed in the Physical Property Measurement System PPMS 14 from the Quantum Design Company[6] in the Joint Laboratory for Magnetic Studies of the Institute of Physics of the Czech Academy of Sciences (CAS) and Charles University in Prague. The PPMS 14 allows experiments at high magnetic fields in the range from −14 T to +14 T with a maximum field error of 12 mT[7] and at temperatures from cryogenic up to 127 °C with an accuracy of ±1% of the temperature measurement.

The Hall sensors were manufactured by the Institute of Plasma Physics of the CAS in Prague within the production batch M10.

The sensors were installed on a heated sample desk dubbed "puck" (Fig. 4). The wiring diagram presented in Fig. 5 enabled the determination of the Hall voltage and magnetoresistance by independent measurements of the transversal resistivity and longitudinal resistivity, respectively.

The properties of the sensors were studied in the magnetic field ranging from −12 to 12 T and the temperature range from

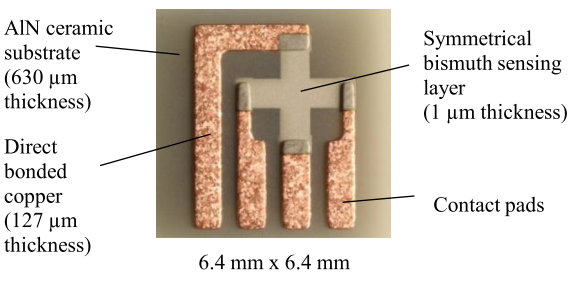

FIG. 3. ITER Hall sensor.

FIG. 4. Resistivity sample puck with the installed Hall sensor.

27 to 127 °C. The magnetic field range was divided into 121 steps and the temperature range was divided into 11 steps, giving a measurement grid of 1331 points, as shown in Fig. 6. The sensor plane was oriented perpendicularly to the magnetic field, and the DC method was used for the Hall voltage measurement.[8] The sensors were powered with a constant DC current of 4 mA, and the output voltage was read by a 20-bit delta-sigma A/D converter.

III. RESULTS

The sensor output voltage dependence on the magnetic field B is shown in Fig. 7.

The same non-linear dependence as in the past measurements[5,8] was detected. Consequently, Fig. 8 shows the dependence of the output voltage on temperature. In accordance with Eq. (1), the observed nonlinearities can be re-expressed in terms of the B- and T-dependent Hall coefficient R_H.[5]

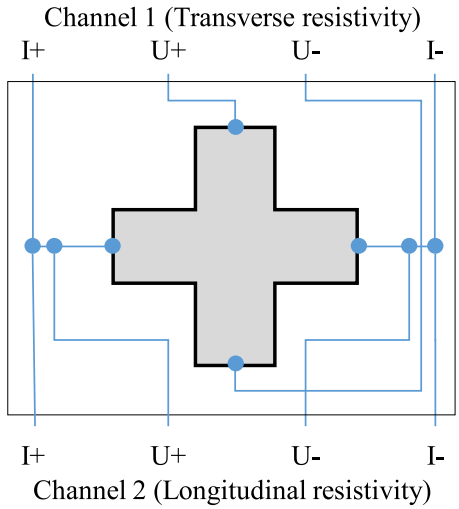

FIG. 5. Wiring diagram of electrical connections to the sensor.

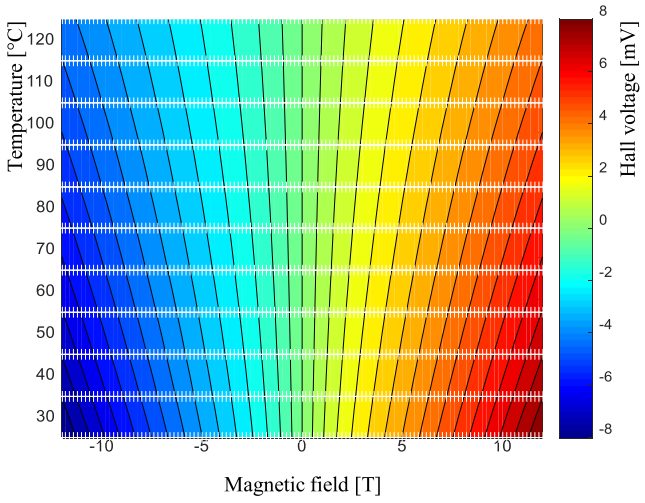

FIG. 6. Measurement grid. White crosses indicate the measurement points, whereas the coloured background denotes a magnitude of the measured Hall voltage ($I = 4$ mA).

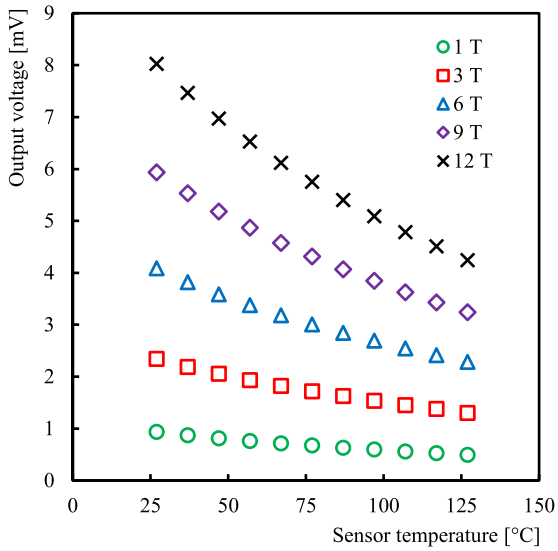

FIG. 8. Hall voltage of the tested bismuth Hall sensors as a function of temperature for various values of the magnetic field ($I = 4$ mA).

Figure 9 shows the Hall coefficient dependence on the magnetic field. From an empirical point of view, $R_H(B)$ can be fitted with a good precision by the sum of three Gaussian functions,

$$R_H(B) = \sum_{i=1}^{3} a_i \exp\left(-(b_i B)^2\right) + c, \tag{2}$$

where a_i, b_i, and c are the fit parameters. The relative error of the fit is less than 0.2% for the tested range of the magnetic field and temperature and less than 0.11% for the sensor operating range.

The Hall coefficient also strongly depends on temperature (Fig. 10). Since semimetallic bismuth should behave similarly to semiconductors (with n-type doping in T and p-type doping in L-point of the Brillouin zone[9]), an exponential dependence implied by the Boltzmann distribution can be expected.[10] The Hall coefficient R_H reduces to $1/ne$ in the single-component limit ($\mu_2 = 0$), where n is the carrier concentration, so that good quality fits to the Hall coefficients data are in the form of the exponential function

$$R_H(T) = k \exp\left(\frac{l}{T+m}\right) + o. \tag{3}$$

The fits with fitting parameters k, l, m, and o are shown in Fig. 10. A relative error of the fits is less than 0.12% for the tested range of the magnetic field and temperature and less than 0.08% for the sensor operating range.

In order to estimate the free charge carrier mobility, the longitudinal resistivity of the sensor supply branch was measured alternately with the sensor supply. The usual positive magnetoresistance was found (see Fig. 11). Resistivity decreasing with temperature shown in Fig. 12 is consistent with thermal activation of free charge carriers.[11]

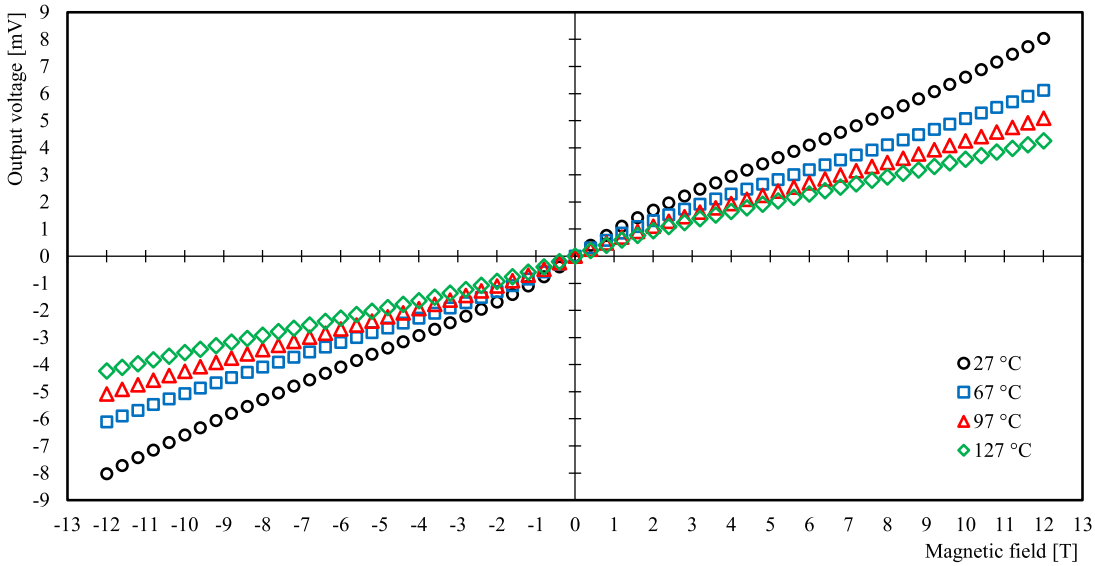

FIG. 7. Hall voltage of the tested bismuth Hall sensors at different temperatures ($I = 4$ mA).

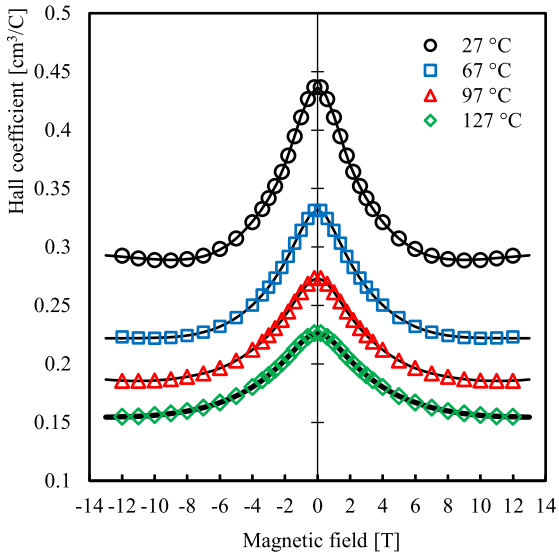

FIG. 9. Hall coefficient as a function of the magnetic field for the tested range of temperatures. Symbols: measurements. Full line: fit Eq. (2).

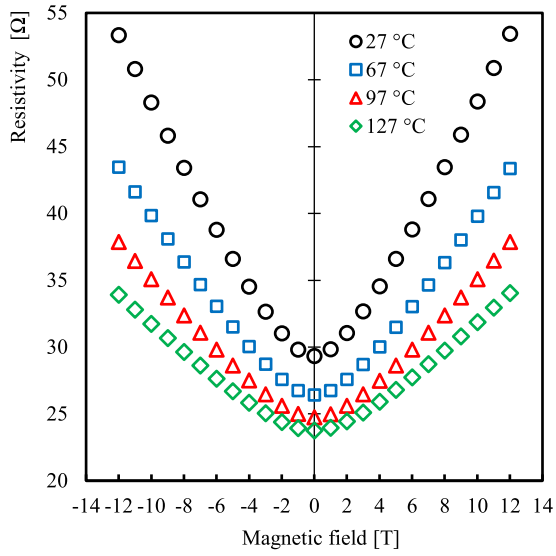

FIG. 11. Longitudinal resistivity of the sensor supply branch as a function of the magnetic field.

IV. DISCUSSION

Although the Gaussian-like fit [Eq. (2)] quality (see Fig. 9) is high for the tested Hall sensors, the equation should be viewed only as a technically convenient expression for fitting since it represents the approximation of a complex dependence coming from solid state physics. Therefore, an alternative expression based on the physical understanding of transport in semimetals was derived.

The sensors contain a thin layer of bismuth, and their morphology[12] is clearly that of a polycrystal. Disregarding the influence of grain boundaries on transport,[13] it can be assumed that the random orientation of grains effectively averages out the multi-component character of carriers[14] into just two components that would naturally correspond to electrons and holes.

In-plane transport in such a model is described by the 2×2 specific conductivity tensor σ whose diagonal components $\sigma_L = \sigma_1/(1 + x^2) + \sigma_2/(1 + y^2)$ are equal, and the two off-diagonal components $\pm\sigma_H$ are equal up to sign, $\sigma_H = \sigma_1 x/(1 + x^2) + \sigma_2 y/(1 + y^2)$. Four parameters are involved, $\sigma_{1,2}$ are the zero-field specific conductivities of the two components, and $\mu_{1,2}$ are their mobilities appearing in $x = \mu_1 B$ and $y = \mu_2 B$, respectively.

The measured Hall coefficient $R_H(B) = \rho_{xy}/B$ is obtained from the specific resistivity tensor $\rho = \sigma^{-1}$. A normalised Hall coefficient can then be fitted to

$$\frac{R_H(B)}{R_H(0)} = \frac{\sigma_H/\sigma_L}{1 + (\sigma_H/\sigma_L)^2} \cdot \frac{(1+s)^2}{\left(\frac{1}{1+x^2} + \frac{s}{1+y^2}\right) \cdot (x + sy)}, \quad (4)$$

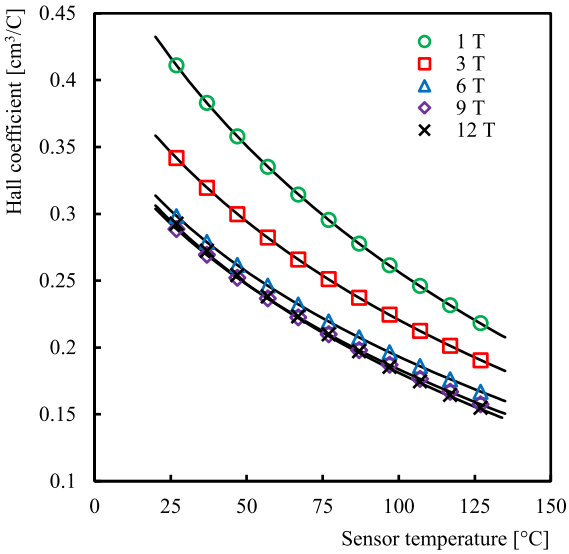

FIG. 10. Hall coefficient as a function of the sensor temperature for B = 1-12 T. Symbols: measurements; lines: fit Eq. (3).

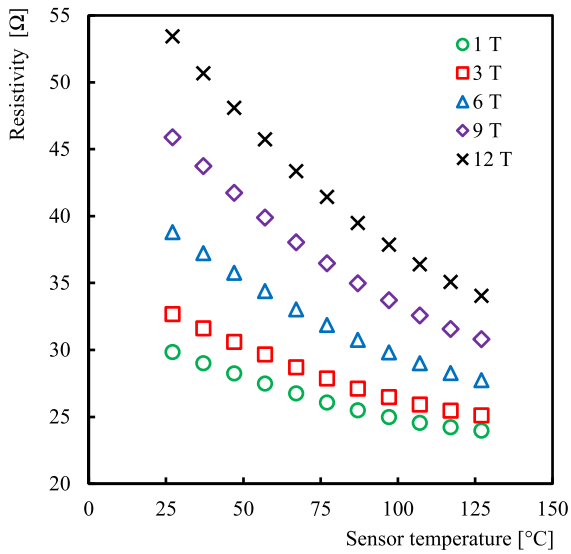

FIG. 12. Longitudinal resistivity of the sensor supply branch as a function of the sensor temperature.

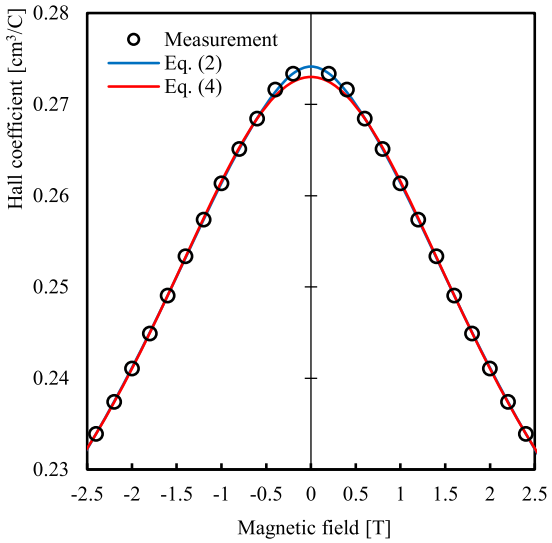

FIG. 13. Hall coefficient as a function of the magnetic field for the sensor operating range of magnetic field ±2.5 T at the temperature of 97 °C.

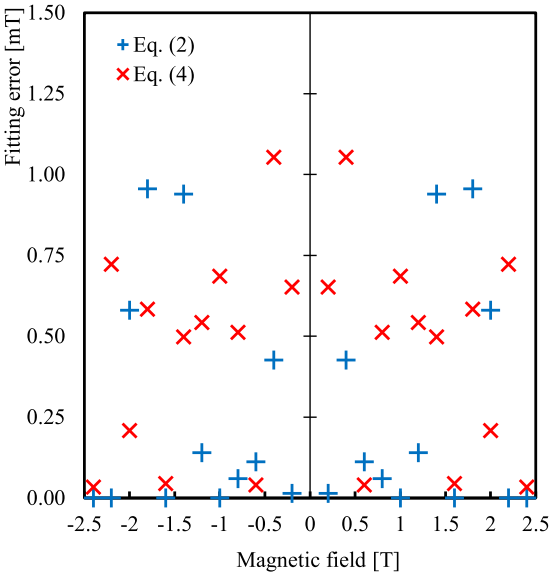

FIG. 14. Fitting error in the magnetic field measurement at the sensor operating range of magnetic field ±2.5 T at the temperature of 97 °C.

where

$$\frac{\sigma_H}{\sigma_L} = \frac{\left[x\left(1+y^2\right)+sy\left(1+x^2\right)\right]}{\left[1+y^2+s\left(1+x^2\right)\right]}. \tag{5}$$

Formula (4) contains three fitting parameters: μ_1, μ_2, and $s = \sigma_2/\sigma_1$. Figure 13 shows a fit to Hall coefficient data in the sensor operating conditions with $s = 0.7924$, $\mu_1 = 0.1773$ 1/T, and $\mu_2 = 0.596$ 1/T. It is possible to fit the data with many other choices of parameters s and $\mu_{1,2}$, while the quality of the fit remains similar to the Gaussian-like Eq. (2) and the physical meaning of the fit parameters is the averaged mobility and conductivity (in the case of s) of the two dominant components of the electron gas.

The analytic equation (4) does not match the data at low magnetic fields accurately. The reason for this discrepancy may be the simplifying assumptions of the free charge carrier transport description. Nevertheless, the fitting error of both the fits, according to Eqs. (2) and (4), is similar in terms of the magnetic field measurement and less than 1.2 mT, as shown in Fig. 14. As a result, the accuracy of the fitting functions has been identified to meet the ITER measurement accuracy requirements.

V. CONCLUSION

The bismuth Hall sensor has been extensively tested for the range of magnetic field and temperature exceeding the sensor operating conditions in ITER. For the first time, the sensors were tested simultaneously at the high magnetic field and at high temperatures. The sensors have proven to be fully functional.

Based on the measurements of the transverse and longitudinal resistivity, the dependency of the Hall voltage and the Hall coefficient of the sensors on the magnetic field and temperature was identified. For this dependency, analytical fitting functions were found and their physical interpretation was discussed.

ACKNOWLEDGMENTS

This work has been partially carried out within the framework of the EUROfusion Consortium and has received funding from the EURATOM research and training programme 2014-2018 under Grant Agreement No. 633053 co-funded by MEYS Project No. 8D15001 and from Project No. CZ.02.1.01/0.0/0.0/16_019/0000768. The experiment was performed in the Materials Growth and Measurement Laboratory, MGML (http://mgml.eu).

The views and opinions expressed herein do not necessarily reflect those of the ITER Organization and the European Commission.

[1]G. Vayakis *et al.*, Rev. Sci. Instrum. **83**, 10D712 (2012).
[2]M. Kocan *et al.*, Fusion Eng. Des. **123**, 936 (2017).
[3]S. Entler *et al.*, IEEE Trans. Plasma Sci. **46**(5), 1276–1280 (2018).
[4]S. Entler *et al.*, Fusion Eng. Des. **123**, 783 (2017).
[5]S. Entler *et al.*, J. Instrum. **12**, C07007 (2017).
[6]See https://www.qdusa.com/ for information about the Quantum Design Company.
[7]Quantum Design: Application Note 1070-207, Rev. A0, June 2009.
[8]I. Duran *et al.*, Rev. Sci. Instrum. **87**, 11D446 (2016).
[9]I. Aguilera *et al.*, Phys. Rev. B **91**, 125129 (2015).
[10]N. W. Ashcroft and N. D. Mermin, in *Solid State Physics* (Harcourt College Publishers, 1976), Chap. 28.
[11]J. S. Kim, J. Appl. Phys. **86**, 3187 (1999).
[12]I. Duran *et al.*, Fusion Eng. Des. **123**, 690 (2017).
[13]P. R. Wallace *et al.*, Solid State Commun. **44**, 873 (1982).
[14]Collaboration, Authors and Editors, "Bismuth (Bi) carrier concentrations and mobilities," Landolt-Börnstein - Group III Condens. Matter **41C**, 1–11 (1998).